

The journal has had 5 points in Ministry of Science and Higher Education parametric evaluation. § 8. 2) and § 12. 1. 2) 22.02.2019.

© The Authors 2021;

This article is published with open access at Licensee Open Journal Systems of Nicolaus Copernicus University in Torun, PolandOpen Access. This article is distributed under the terms of the Creative Commons Attribution Noncommercial License which permits any noncommercial use, distribution, and reproduction in any medium, provided the original author (s) and source are credited. This is an open access article licensed under the terms of the Creative Commons Attribution Non commercial license Share alike.(<http://creativecommons.org/licenses/by-nc-sa/4.0/>) which permits unrestricted, non commercial use, distribution and reproduction in any medium, provided the work is properly cited. The authors declare that there is no conflict of interests regarding the publication of this paper.

Received: 10.07.2021. Revised: 20.07.2021. Accepted: 31.07.2021.

Immediate effects of Ukrainian phytocomposition on biophotonics (GDV), EEG and HRV parameters

Oksana A. Fihura¹, Sofiya V. Ruzhylo¹, Xawery Żukow², Igor L. Popovych³

¹Ivan Franko Pedagogical University, Drohobych, Ukraine
doctor-0701@ukr.net oksanafigura08@gmail.com

²Medical University of Białystok, Białystok, Poland xaweryzukow@gmail.com

³Bohomolets' Institute of Physiology of National Academy of Sciences, Kyiv, Ukraine
i.popovych@biph.kiev.ua

Background. Back in 2015, we registered short-term reactions to the Ukrainian phytocomposition of electroencephalogram and heart rate variability parameters. At the same time, we also recorded the reactions of biophotonics (GDV) parameters, but due to the skepticism of Ukrainian academic science regarding this method, we did not dare to include the results in the article. **Materials and methods.** The object of observation were 12 women (44 ± 13 years) and 62 men (44 ± 12 years) with dysfunction of neuro-endocrine-immune complex. GDV, HRV and EEG parameters were recorded in the morning in basal conditions. Then the members of the main group used 5 ml of phytocomposition dissolved in 45 ml of tap water, instead in the control group used 50 ml of the latter. After 1,5 hours, the test was repeated. **Results.** Discriminant analysis revealed 26 EEG, 6 HRV and 7 GDV parameters characteristic of the initial state and after consumption of phytocomposition or tap water. The use of balm causes the normalizing decrease of increased sympathotonic markers and the increase of decreased vagotonic markers. Physiologically favorable vegetotropic effects of the balm are accompanied by a further increase in the initially increased activity of β -rhythm-generating cortical and subcortical structures as well as activation of θ -rhythm-generating and inhibition of α - and δ -rhythm-generating nuclei whose initial activity was within normal limits. Neurotropic effects are accompanied by a decrease in fractality and entropy and an increase in the area of GDI, as well as the energy of the first, fourth, fifth and seventh chakras (virtual).

Conclusion. Ukrainian phytocomposition “Balm Truskavets” causes favorable immediate neurotropic and biophysic changes at patients with dysfunction of neuro-endocrine-immune complex.

Keywords: phytocomposition “Balm Truskavets”, GDV, EEG, HRV, immediate effects.

INTRODUCTION

Back in 2015, we registered short-term reactions to the Ukrainian phytocomposition of electroencephalogram and heart rate variability parameters of almost healthy volunteers [50]. At the same time, we also recorded the reactions of biophotonics parameters, but due to the skepticism of Ukrainian academic science regarding this method, we did not dare to include the results in the article. But, as the ancient Romans said, “*tempora mutantur et nos mutamur cum illis*”. After the publication of the article we have been shown that exist strong canonical correlation between parameters of gas discharge visualization (GDV) and principal neuroendocrine factors of adaptation [2] as well as parameters of EEG [3], leukocytogram [6], immunity [4] and phagocytosis [5]. The obtained data gave us irrefutable arguments for a substantive discussion with potential opponents about the relevance of the method.

Recall that the GDV (kirlianography, biophotonics) method is based on the registration of stimulated emission of photons and electrons from the skin surface. Korotkov KG [22-24] believes that GDV method measures the distribution of electron densities in human systems and organs. These electron densities are the main basis of physiological energy, so there is reason to say that the GDV method allows us to measure the body's potential energy reserve. At the same time, the GDV method is a bridge between the logical science of the West and the intuitive science of the East. It allows us to represent the same phenomena in different languages, in different systems, to look at the same things from different points of view.

According to Ayurvedic medicine, Chakras are power centers, related to the endocrine glands and neural plexus as well as to some organs. In Puchko LG [48] we read that the **first** Chakra is related to the testicles and sacral plexus, **second** Chakra to the ovaries, adrenals and kidneys, **third** Chakra to **spleen**, liver and solar plexus, **fourth** Chakra to **thymus**, heart and cardiac plexus, **fifth** Chakra to thyroid and parathyroid glands, **sixth** Chakra to pituitary gland and brain, **seventh** Chakra to pineal gland. Chase CR [10] provides a table according to which the **first** Chakra is associated with adrenals, pelvic nerve plexus, spine, kidneys, bladder, large intestine; **second** Chakra with testes/ovaries, inferior mesenteric ganglion, ileum, organs of reproduction; **third** Chakra with [endocrine] pancreas, celiac plexus ganglion, liver, gall bladder, stomach, duodenum, pancreas, **spleen**; **fourth** Chakra with **thymus**, celiac plexus, heart, circulation, vagus nerve; **fifth** Chakra with thyroid and parathyroid glands, inferior cervical ganglion, lungs, bronchus, larynx, pharynx, large intestine, vagus nerve; **sixth** Chakra with pituitary and pineal glands, thalamus, hypothalamus, superior cervical ganglion, left brain, lower brain, ears/nose, left eye; **seventh** Chakra with pineal gland, right brain, upper brain, right eye.

Korotkov KG [23] put forward the concept that each Chakra is associated with a part of the finger. This approach is embodied in the “GDV Chakras” program, which allows us to quantify the state of *virtual* Chakras.

MATERIAL AND METHODS

The object of observation were 12 women (44 ± 13 years) and 62 men (44 ± 12 years) with dysfunction of neuro-endocrine-immune complex, employees of the clinical sanatoria “Kryshťalevý Palats” and “Moldova” (Truskavets’, Ukraine). Every morning before work, carried out initial tests of 6 persons, then the two of them (basic group) used 5 ml of phytocomposition “Balm Truskavets” (TY Y 15.8-24055046-005:2009, produced by private research and production enterprise “Ukrainian Balms”, Mykolayiv, Ukraine), pre-diluted in 45 ml of boiled tap water. This phytocomposition is analogous to the previous “Balm Kryms’kyi”. The other 4 individuals (control group) used 50 ml of the same water at room temperature (CW).

In the morning on an empty stomach we registered kirlianogram by the method of GDV by the device of “GDV Chamber” (“Biotechprogress”, SPb, RF). The first base parameter of GDV

is **Area** of gas discharge image (GDI) in Right, Frontal and Left projections. The second base parameter is a **Shape coefficient** (ratio of square of length of external contour of GDI toward his Area), which characterizes the measure of serration/fractality of external contour. The third base parameter of GDI is **Entropy**, id est measure of chaos. Program estimates also **Energy** and **Asymmetry** of virtual **Chakras** [22-24].

To assess the parameters of heart rate variability (HRV) recorded during 7 min electrocardiogram in II lead (software and hardware complex "CardioLab+HRV", KhAI-MEDICA, Kharkiv). For further analysis the following parameters HRV were selected. Temporal parameters (Time Domain Methods): the standard deviation of all NN intervals (SDNN), the square root of the mean of the sum of the squares of differences between adjacent NN intervals (RMSSD), the percent of interval differences of successive NN intervals greater than 50 msec (pNN₅₀); Triangular Index (TNN). Spectral parameters (Frequency Domain Methods): power spectral density (PSD) bands of HRV - high-frequency (HF, range 0,40÷0,15 Hz), low-frequency (LF, range 0,15÷0,04 Hz), very low-frequency (VLF, range 0,040÷0,015 Hz) and ultralow-frequency (ULF, range 0,015÷0,003 Hz). Calculated classical indexes: LF/HF; (VLF+LF)/HF; LFnu=100%•LF/(LF+HF) [7,9,14].

After 8-13 minutes, the EEG recorded a hardware-software complex "NeuroCom Standard" (KhAI MEDICA, Kharkiv) monopolar in 16 loci (Fp1, Fp2, F3, F4, F7, F8, C3, C4, T3, T4, P3, P4, T5, T6, O1, O2) by 10-20 international system, with the reference electrodes A and Ref on the lobes of the ears. The duration of the epoch was 25 sec. Among the options considered the average EEG amplitude (μ V), average frequency (Hz), frequency deviation (Hz), index (%) as well as absolute (μ V²/Hz) and relative (%) PSD of basic rhythms: β (35÷13 Hz), α (13÷8 Hz), θ (8÷4 Hz) and δ (4÷0,5 Hz) in all loci, according to the instructions of the device. In addition, calculated coefficient of Asymmetry (As) and Laterality Index (LI) for PSD each Rhythm using formulas [35]:

$$As, \% = 100 \cdot (Max - Min) / Min;$$

$$LI, \% = \Sigma [200 \cdot (Right - Left) / (Right + Left)] / 8.$$

We calculated also for each locus EEG and HRV Shannon's CE [53] Entropy (h) of normalized PSD using Popovych's [13,50] formulas:

$$h_{EEG} = - [PSD\alpha \cdot \log_2 PSD\alpha + PSD\beta \cdot \log_2 PSD\beta + PSD\theta \cdot \log_2 PSD\theta + PSD\delta \cdot \log_2 PSD\delta] / \log_2 4$$

$$h_{HRV} = - [PSHF \cdot \log_2 PSHF + PSLF \cdot \log_2 PSLF + PSVLF \cdot \log_2 PSVLF + PSULF \cdot \log_2 PSULF] / \log_2 4$$

HRV reference values were taken from the instructions for the "CardioLab+HRV" device, GDV and EEG references were taken from the database of Truskavetsian Scientific School of Balneology.

RESULTS AND DISCUSSION

In order to identify among the registered parameters those whose constellation is three states of persons: initial and after the use of a solution of phytocomposition or control water - differ significantly from each other, discriminant analysis was used [20]. The forward stepwise program included 39 variables in the discriminant model (Tables 1 and 2). Among them, 2 relate to **delta-rhythm**, 4 - **theta-rhythm**, 9 - **alpha-rhythm**, 10 - **beta-rhythm**, 1 - **entropy** of EEG, and the other 6 – HRV, including 2 **sympathetic** and 3 **vagal** markers as well as **entropy** of HRV bands. However, we are most interested in the 7 parameters of **biophotonics**, which confirms their relationship with the parameters of EEG and HRV.

Table 1. Discriminant Function Analysis Summary for GDV, EEGs and HRVs Variables as well as their Reference levels and Coefficients of Variability

Step 39, N of vars in model: 39; Grouping: 3 grps; Wilks' Λ : 0,199; approx. $F_{(78)}=3,4$; $p<10^{-6}$

Variables currently in the model (n=148)	Groups (n)			Parameters of Wilks' Statistics						Reference Cv/SD
	After Balm (20)	Base-line (74)	After CW (54)	Wilks' Λ	Partial Λ	F-remove (2,1)	p-level	Tolerance		
Area GDI Right, kpixels	29,41 0,68	27,04 0,56	27,02 0,65	0,206	0,968	1,75	0,178	0,060	27,02 0,151	
Shape Coefficient GDI Right	14,2 0,5	16,9 0,8	16,9 0,8	0,215	0,925	4,35	0,015	0,054	17,2 0,331	
Shape Coefficient GDI Frontal	19,1 1,2	22,1 1,3	23,3 1,5	0,217	0,920	4,63	0,012	0,065	23,4 0,395	
Chakra 1 Energy	0,35 0,06	0,23 0,04	0,16 0,06	0,213	0,938	3,56	0,032	0,156	0,20 0,34	
Chakra 2 Asymmetry	0,20 0,07	-0,02 0,05	0,21 0,06	0,201	0,989	0,58	0,561	0,431	0,22 0,38	
Chakra 5 Energy	0,27 0,07	0,11 0,03	0,13 0,04	0,215	0,925	4,33	0,016	0,316	0,12 0,23	
Chakra 7 Energy	0,13 0,06	0,03 0,03	-0,01 0,04	0,203	0,980	1,07	0,346	0,192	0,04 0,26	
ULF/TP HRV, %	2,3 0,7	6,8 0,8	10,4 1,2	0,230	0,867	8,24	10^{-3}	0,337	4,6 0,674	
LF/HF HRV	3,45 0,85	4,04 0,33	5,21 0,41	0,201	0,990	0,53	0,593	0,288	2,80 0,714	
HF HRV PSD, msec²	468 174	291 61	145 15	0,200	0,996	0,20	0,818	0,064	452 0,768	
RMSD HRV, msec	26,4 4,2	23,5 1,5	19,2 1,0	0,214	0,929	4,08	0,020	0,091	37,0 0,459	
pNN₅₀ HRV, %	8,3 3,7	5,4 1,2	2,6 0,4	0,205	0,973	1,48	0,233	0,037	9,0 0,858	
P4-δ PSD, %	14,3 1,7	20,2 1,3	19,4 1,6	0,223	0,892	6,45	0,002	0,186	27,1 0,671	
P4-δ PSD, μV²/Hz	47 8	79 9	95 11	0,229	0,871	7,92	0,001	0,152	107 0,886	
Asymmetry-θ, %	28,6 3,7	23,0 2,1	18,1 1,8	0,204	0,975	1,37	0,258	0,467	23,0 0,699	
O1-θ PSD, %	9,0 1,3	6,6 0,5	6,0 0,5	0,204	0,977	1,28	0,283	0,182	6,7 0,636	
O1-θ PSD, μV²/Hz	24 4	36 5	38 5	0,203	0,983	0,91	0,405	0,227	36 1,213	
O2-θ PSD, %	7,1 1,0	5,2 0,3	5,0 0,4	0,202 593	0,984	0,89	0,412	0,491	6,0 0,603	
Fp1-α PSD, %	27,1 2,5	37,7 2,3	39,7 2,7	0,206	0,966	1,91	0,153	0,089	37,2 0,501	
F3-α PSD, %	24,2 2,2	35,7 2,2	41,4 2,3	0,206	0,966	1,89	0,156	0,038	34,5 0,547	
F3-α PSD, μV²/Hz	85 11	156 20	183 24	0,220	0,904	5,69	0,004	0,057	146 1,071	
T3-α PSD, %	24,0 2,0	31,6 1,9	36,2 2,0	0,205	0,972	1,54	0,219	0,064	30,7 0,546	
T3-α PSD, μV²/Hz	62 8	104 13	119 15	0,205	0,970	1,66	0,196	0,107	97 0,988	
C3-α PSD,	26,4	35,4	42,4	0,214	0,932	3,89	0,023	0,043	35,3	

%	2,2	2,1	2,3						0,510
T6-α PSD, %	23,5 2,7	33,6 2,4	37,3 2,9	0,207	0,962	2,09	0,128	0,095	32,2 0,623
O2-α PSD, %	38,6 4,4	45,5 3,0	50,1 3,5	0,203	0,982	0,98	0,377	0,071	44,6 0,532
O2-α PSD, $\mu\text{V}^2/\text{Hz}$	229 84	463 79	697 128	0,225	0,884	7,03	0,001	0,104	410 1,627
Frequency-β, %	17,2 0,8	19,6 0,5	20,0 0,5	0,215	0,929	4,11	0,019	0,570	19,0 0,200
Asymmetry-β, %	21,7 4,3	23,9 2,1	17,6 2,8	0,211	0,945	3,11	0,049	0,610	20,1 0,699
F3-β PSD, $\mu\text{V}^2/\text{Hz}$	108 10	83 7	69 6	0,208	0,960	2,22	0,113	0,128	78 0,667
T4-β PSD, %	42,5 4,3	36,7 2,1	30,6 2,3	0,212	0,938	3,55	0,032	0,088	27,9 0,591
C4-β PSD, %	38,9 3,2	30,9 1,8	25,8 2,1	0,210	0,951	2,76	0,068	0,098	26,3 0,493
C4-β PSD, $\mu\text{V}^2/\text{Hz}$	122 12	89 7	71 5	0,228	0,874	7,69	0,001	0,072	84 0,671
T4-β PSD, $\mu\text{V}^2/\text{Hz}$	99 10	88 10	64 4	0,232	0,859	8,81	10^{-3}	0,177	72 0,745
T6-β PSD, %	49 5	40 2	26 3	0,214	0,931	3,96	0,022	0,098	30 0,646
P3-β PSD, %	41,6 3,7	30,2 1,8	26,8 2,1	0,209	0,951	2,73	0,070	0,100	25,0 0,549
O1-β PSD, %	42,3 4,7	36,1 2,5	31,1 2,9	0,205	0,973	1,48	0,233	0,106	26,7 0,656
Entropy PSD HRV	0,728 0,025	0,766 0,012	0,785 0,013	0,205	0,970	1,63	0,201	0,273	0,825 0,114
Entropy EEG PSD in O1	0,798 0,036	0,718 0,021	0,709 0,023	0,207	0,961	2,17	0,119	0,190	0,738 0,245

Note. For groups the average values and standard errors are specified; for the norm - the average values and coefficients of variation (Cv) or standard deviations (SD).

Table 2. Summary of Stepwise Analysis for GDV, EEGs and HRVs Variables. The variables are ranked by criterion Lambda

Variables currently in the model	F to enter	p-level	Λ	F-value	p-level
ULF/TP, %	10,8	10^{-4}	0,871	10,8	10^{-4}
F3-α PSD, %	8,05	0,0005	0,783	9,36	10^{-6}
P4-δ PSD, %	9,22	0,0002	0,694	9,56	10^{-6}
C4-β PSD, $\mu\text{V}^2/\text{Hz}$	5,79	0,0038	0,641	8,83	10^{-6}
Chakra 2 Asymmetry	4,52	0,0125	0,603	8,12	10^{-6}
T4-β PSD, $\mu\text{V}^2/\text{Hz}$	4,87	0,0090	0,564	7,75	10^{-6}
Fp1-α PSD, %	3,71	0,0270	0,535	7,29	10^{-6}
P4-δ PSD, $\mu\text{V}^2/\text{Hz}$	3,22	0,0431	0,511	6,88	10^{-6}
LF/HF	3,01	0,0527	0,490	6,53	10^{-6}
Asymmetry-β, %	3,27	0,0409	0,467	6,30	10^{-6}
O2-θ PSD, %	3,12	0,0474	0,447	6,09	10^{-6}
Frequency-β, %	2,56	0,0810	0,430	5,86	10^{-6}
O1-θ PSD, $\mu\text{V}^2/\text{Hz}$	1,72	0,1830	0,419	5,57	10^{-6}
C3-α PSD, %	1,77	0,1738	0,408	5,33	10^{-6}

Chakra 5 Energy	1,64	0,1970	0,398	5,10	10^{-6}			
T6-α PSD, %	2,16	0,1196	0,385	4,96	10^{-6}			
C4-β PSD, %	2,72	0,0698	0,370	4,89	10^{-6}			
P3-β PSD, %	2,33	0,1016	0,357	4,79	10^{-6}			
Entropy HRV	2,73	0,0694	0,342	4,74	10^{-6}			
HF HRV PSD, msec²	1,87	0,1587	0,332	4,63	10^{-6}			
Chakra 1 Energy	1,83	0,1640	0,323	4,52	10^{-6}			
T3-α PSD, μV²/Hz	1,64	0,1981	0,315	4,41	10^{-6}			
F3-α PSD, μV²/Hz	1,75	0,179	0,306	4,32	10^{-6}			
O2-α PSD, μV²/Hz	1,73	0,1816	0,297	4,24	10^{-6}			
O2-α PSD, %	1,86	0,1607	0,289	4,17	10^{-6}			
T6-β PSD, %	1,89	0,1560	0,280	4,11	10^{-6}			
T4-β PSD, %	2,33	0,1018	0,269	4,09	10^{-6}			
RMSSD HRV, msec	1,15	0,3192	0,264	3,99	10^{-6}			
pNN₅₀ HRV, %	1,37	0,2589	0,258	3,91	10^{-6}			
F3-β PSD, μV²/Hz	1,19	0,3067	0,253	3,82	10^{-6}			
Asymmetry-0, %	1,28	0,2808	0,247	3,75	10^{-6}			
Shape Coef GDI Right	1,46	0,2373	0,241	3,69	10^{-6}			
Shape Coe GDI Frontal	2,92	0,0578	0,229	3,73	10^{-6}			
O1-β PSD, %	1,42	0,2449	0,224	3,67	10^{-6}			
Area GDI Right, pixels	1,36	0,2617	0,218	3,62	10^{-6}			
T3-α PSD, %	1,46	0,2372	0,213	3,57	10^{-6}			
Entropy EEG O1	1,16	0,3180	0,208	3,51	10^{-6}			
O1-0 PSD, %	1,32	0,2717	0,203	3,46	10^{-6}			
Chakra 7 Energy	1,07	0,3457	0,199	3,40	10^{-6}			

In addition, a number of other GDV, EEG and HRV parameters that were not included in the model are noteworthy (Table 3).

Table 3. Discriminant Function Analysis Summary for GDV, EEG and HRV Variables currently not in the model

Variables	Groups (n)			Parameters of Wilks' Statistics					Reference Cv/SD
	After Balm (20)	Base-line (74)	After CW (54)	Wilks' Λ	Partial Λ	F to enter	p-level	Tole-rancy	
Entropy GDI Right	3,75 0,04	3,86 0,03	3,88 0,03	0,199	0,998	0,09	0,911	0,333	3,86 0,052
Chakra 3 Asymmetry	0,37 0,10	0,18 0,05	0,25 0,06	0,199	0,994	0,19	0,894	0,333	0,22 0,38
Chakra 4 Energy	0,51 0,03	0,39 0,04	0,34 0,06	0,196	0,982	0,97	0,382	0,277	0,40 0,28
LFnu, %	64,7 4,8	72,9 1,9	79,5 1,5	0,198	0,993	0,38	0,683	0,165	61,8 0,247
HF/TP, %	20,9 3,9	14,0 1,3	9,3 0,5	0,199	0,996	0,20	0,820	0,151	17,1 1,230
Frequency-δ, Hz	1,08 0,04	1,09 0,02	1,03 0,02	0,199	0,997	0,15	0,860	0,596	1,07 0,165
Deviation-0, Hz	1,25 0,14	1,11 0,08	0,94 0,08	0,199	0,999	0,03	0,973	0,701	1,00 0,616
Amplitude-α, μV	13,9 1,9	17,8 1,5	20,9 2,1	0,197	0,988	0,63	0,536	0,030	17,7 0,703
Index α, %	34,1 6,2	42,9 4,0	47,7 4,4	0,197	0,988	0,65	0,526	0,193	48,4 0,558
Fp1-α PSD,	63	120	140	0,197	0,986	0,73	0,483	0,025	109

μV²/Hz	9	15	18						1,063
Fp2-α PSD, %	27,5 2,4	35,3 2,2	37,3 2,5	0,199	1,000	0,01	0,991	0,188	33,2 0,535
F4-α PSD, %	25,8 2,2	34,7 2,2	41,7 2,4	0,199	0,997	0,18	0,833	0,073	32,7 0,564
F4-β PSD, %	32,4 3,5	29,9 1,9	25,2 1,9	0,199	0,998	0,08	0,920	0,158	24,5 0,544
F7-α PSD, μV²/Hz	97 3	56 8	63 9	0,198	0,994	0,30	0,744	0,149	59 1,410
T6-α PSD, μV²/Hz	49 6	102 15	124 18	0,196	0,983	0,93	0,399	0,147	100 1,397
O1-α PSD, %	32,7 3,1	40,7 3,0	46,3 3,4	0,199	0,998	0,11	0,894	0,059	39,9 0,591
Entropy EEG PSD in O2	0,760 0,029	0,688 0,018	0,666 0,022	0,199	0,996	0,19	0,827	0,141	0,727 0,242

Next, the 39-dimensional space of discriminant variables transforms into 2-dimensional space of canonical roots. The canonical correlation coefficient is for Root 1 0,770 (Wilks' $\Lambda=0,223$; $\chi^2_{(68)}=193$; $p<10^{-6}$), for Root 2 0,673 (Wilks' $\Lambda=0,547$; $\chi^2_{(33)}=78$; $p<10^{-4}$). The major root contains 63,7% of discriminative opportunities, the minor - 36,3%.

Table 4 presents raw (actual) and standardized (normalized) coefficients for discriminant variables. The calculation of the discriminant root values for each person as the sum of the products of raw coefficients to the individual values of discriminant variables together with the constant enables the visualization of each person in the information space of the roots.

Table 4. Standardized and Raw Coefficients and Constants for Canonical GDV, EEGs and HRVs Variables

Coefficients	Standardized		Raw		
	Variables	Root 1	Root 2	Root 1	Root 2
ULF/TP, %	0,650	-0,546	0,094	-0,079	
F3-α PSD, %	0,656	0,808	0,038	0,047	
P4-δ PSD, %	0,798	0,629	0,071	0,056	
C4-β PSD, μV²/Hz	-1,492	-0,976	-0,030	-0,020	
Ch2 Asymmetry	-0,079	-0,163	-0,286	-0,587	
T4-β PSD, μV²/Hz	0,789	0,931	0,012	0,014	
Fp1-α PSD, %	-0,124	0,331	-0,007	0,020	
P4-δ PSD, μV²/Hz	-0,226	-0,239	-0,079	-0,084	
LF/HF	-0,032	-0,283	-0,011	-0,093	
Asymmetry-β, %	-0,124	-1,185	-0,002	-0,016	
O2-θ PSD, %	0,413	0,109	0,108	0,029	
Frequency-β, %	0,181	0,435	0,005	0,011	
O1-θ PSD, μV²/Hz	-0,197	-2,245	-0,012	-0,132	
C3-α PSD, %	0,819	-0,099	0,054	-0,007	
Ch5 Energy	-0,779	-0,167	-0,049	-0,011	
T6-α PSD, %	-0,416	-0,071	-4,057	-0,689	
C4-β PSD, %	-0,320	-0,585	-1,789	-3,271	
P3-β PSD, %	0,693	-0,007	0,035	-0,0004	
Entropy HRV	0,523	-0,298	0,001	-0,0006	
HF, msec²	0,644	0,157	0,006	0,002	
Ch1 Energy	-0,431	1,482	-0,003	0,009	
T3-α PSD, μV²/Hz	0,022	-1,540	0,00003	-0,0020	
F3-α PSD, μV²/Hz	-0,183	1,319	-0,007	0,053	
O2-α PSD, μV²/Hz	-0,550	-1,358	-0,026	-0,064	

O2- α PSD, %	0,602	0,964	0,034	0,054
T6- β PSD, %	0,508	-0,522	2,933	-3,018
T4- β PSD, %	-0,483	0,346	-0,115	0,082
RMSSD, msec	-0,402	0,581	-0,033	0,048
pNN ₅₀ , %	-0,039	0,803	-0,158	3,243
F3- β PSD, μ V ² /Hz	-0,021	1,524	-0,005	0,373
Asymmetry-θ, %	-0,509	-1,172	-0,076	-0,175
Shape C Right	-0,884	-0,257	-0,0003	-0,00008
Shape C Frontal	-0,032	0,289	-0,002	0,018
O1- β PSD, %	0,367	-0,104	1,958	-0,552
Area GDI R, pixels	0,650	-0,546	0,094	-0,079
T3- α PSD, %	0,656	0,808	0,038	0,047
Entropy O1	0,798	0,629	0,071	0,056
O1-θ PSD, %	-1,492	-0,976	-0,030	-0,020
Ch7 Energy	-0,079	-0,163	-0,286	-0,587
Constants		8,033	2,886	
Eigenvalues		1,457	0,829	
Cumulative Proportion		0,637	1	

Table 5 presents the full structural coefficients, that is, the coefficients of correlation between the discriminant root and variables. The structural coefficient shows what is the proportion of information about the root contained in this variable. There are also average values (centrodes) of Roots and Z-scores of Variables. We consider it expedient to include in the table also out-of-model variables in view of their recognizability.

Table 5. Factor Structure Matrix and Means of Roots and Variables

Variables, Z	Correlations Variables-Roots		After Balm (20)	Base- line (74)	After CW (54)
	R1	R2			
Root 1 (63,8%)	R1	R2	-2,96	+0,25	+0,76
ULF/TP, %	0,281	-0,200	-0,73	+0,70	+1,88
LF/HF	0,128	0,166	+0,33	+0,62	+1,20
LFnu, %			+0,19	+0,73	+1,16
F3- α PSD, %	0,250	-0,104	-0,55	+0,06	+0,36
C3- α PSD, %	0,228	-0,154	-0,50	0,00	+0,39
T6- α PSD, %	0,177	-0,048	-0,43	+0,07	+0,25
F3- α PSD, μ V ² /Hz	0,155	-0,045	-0,39	+0,06	+0,24
O2- α PSD, μ V ² /Hz	0,146	-0,121	-0,27	+0,08	+0,43
O2- α PSD, %	0,113	-0,065	-0,25	+0,04	+0,23
T3- α PSD, %			-0,40	+0,05	+0,33
Fp1- α PSD, μ V ² /Hz			-0,39	+0,10	+0,27
F4- α PSD, %			-0,38	+0,11	+0,49
O1- α PSD, %			-0,31	+0,03	+0,27
Amplitude- α , μ V			-0,31	+0,01	+0,26
Frequency- β , Hz	0,194	-0,010	-0,46	+0,15	+0,27
T3- α PSD, μ V ² /Hz	0,140	-0,033	-0,36	+0,08	+0,22
Fp1- α PSD, %			-0,54	+0,08	+0,14
F7- α PSD, μ V ² /Hz			-0,38	-0,04	+0,05
T6- α PSD, μ V ² /Hz			-0,36	+0,02	+0,17
Fp2- α PSD, %			-0,32	+0,12	+0,23
Index α , %			-0,53	-0,20	-0,03
O1-θ PSD, μ V ² /Hz	0,095	0,005	-0,26	+0,02	+0,05
Shape C GDI Right	0,136	0,031	-0,52	-0,06	-0,05

Shape C GDI Frontal	0,111	-0,019	-0,46	-0,14	-0,01
Entropy GDI Right			-0,50	+0,06	+0,15
P4-δ PSD, μV²/Hz	0,162	-0,067	-0,64	-0,30	-0,13
P4-δ PSD, %	0,133	0,074	-0,71	-0,38	-0,43
Entropy HRV	0,140	-0,056	-1,03	-0,62	-0,43
C4-β PSD, μV²/Hz	-0,262	0,122	+0,69	+0,09	-0,23
F3-β PSD, μV²/Hz			+0,56	+0,08	-0,19
O2-0 PSD, %	-0,200	-0,015	+0,30	-0,23	-0,28
O1-0 PSD, %	-0,185	0,024	+0,52	-0,03	-0,17
Asymmetry-θ, %	-0,153	0,116	+0,35	0,00	-0,30
Deviation-0, Hz			+0,39	+0,16	-0,10
Area GDI Right	-0,170	-0,023	+0,59	+0,01	0,00
Chakra 5 Energy	-0,166	-0,094	+0,65	-0,05	0,04
Chakra 7 Energy	-0,145	0,033	+0,35	-0,05	-0,20
Chakra 1 Energy	-0,132	0,046	+0,43	+0,08	-0,13
Chakra 4 Energy			+0,40	-0,02	-0,22
Entropy EEG O1	-0,139	-0,009	+0,33	-0,11	-0,16
Entropy EEG O2			+0,19	-0,22	-0,34
P3-β PSD, %	-0,243	0,048	+1,21	+0,38	+0,13
C4-β PSD, %	-0,215	0,120	+0,97	+0,36	-0,04
T6-β PSD, %	-0,161	0,064	+0,98	+0,51	+0,29
T4-β PSD, %	-0,157	0,135	+0,89	+0,54	+0,16
T4-β PSD, μV²/Hz	-0,121	0,120	+0,51	+0,30	-0,16
F4-β PSD, %			+0,73	+0,41	+0,05
O1-β PSD, %			+0,94	+0,53	+0,25
HF, msec²	-0,164	0,116	+0,04	-0,46	-0,88
RMSSD, msec	-0,136	0,152	-0,63	-0,79	-1,05
HF/TP, %			+0,18	-0,15	-0,37
pNN₅₀, %			-0,06	-0,47	-0,83
Root 2 (36,3%)	R1	R2	-0,45	+0,88	-1,04
Chakra 2 Asymmetry	-0,086	-0,232	+0,28	-0,39	+0,31
Chakra 3 Asymmetry			+0,40	-0,10	+0,07
Asymmetry-β, %	-0,036	0,185	+0,11	+0,27	-0,18
Frequency-δ, Hz			+0,02	+0,13	-0,25

As a preamble, we present existing views on the interpretation of HRV parameters. Well-known markers of Vagal tone are HF, RMSSD and pNN₅₀. LFnu is admitted HRV marker of Sympathetic tone, LF/HF ratio reflects the sympathetic-vagal balance. It is speculated that absolute PSD LF band reflects mainly Sympathetic outflow or both Sympathetic and Vagal origin [7,9,14,52]. The interpretation of the other two bands remains the most controversial. VLF band (0,040÷0,0033 Hz) associated with oscillation blood levels of renin (0,04 Hz) and epinephrine (0,025 Hz), reflects thermoregulatory cycles, endothelial influences, cerebral ergotropic and metabolotropic outflows, activation of cerebral sympatho-adrenal system, sympathetic and vagal activity [7,18,19,21,25,52]. ULF band (<0,0033 Hz) associated with oscillation blood level of norepinephrine (0,0020 Hz) as well as 17-OCS (0,0019 Hz) [cit by: 25]. Because in our device ULF band (range 0,015÷0,003 Hz) is integrated into the lower zone of VLF band, what has been said about the latter also applies to the former.

The above gives grounds to state in our contingent a sympathotonic shift of the autonomic balance due to both an increase in **sympathetic** tone and a decrease in **vagal** tone. There may be elevated levels of norepinephrine and glucocorticoids in the blood. This is accompanied by **increased** activity of beta-rhythm-generating cortical and subcortical structures that are

designed on the right (paired) loci C4, T4, T6 and F4 as well as left loci P3 and O1. The right-hand shift of beta-rhythm symmetry is documented by a positive value of the asymmetry index. Interestingly, the symmetry of **Chakra 2** and, to a lesser extent, **Chakra 3** is shifted to the left.

It is traditionally believed that loci C3/C4 projected hippocampus, loci T3/T4 reflect the activity of the amygdala [49]. In practice, transcranial magnetic and direct current stimulation of the T3/T4 scalp position is used to reach the insular cortex, and F3/F4 loci - to activate the dorsolateral prefrontal cortex nuclei [review: 16]. The figures presented by Winkelmann T et al [54] and Yoo HJ et al [55] give us reason to assume that the loci C3/C4 projected precentral gyrus, T3/T4 – inferior temporal gyrus, F3/F4 - caudal anterior cingulate cortex or rostral middle frontal gyrus or superior frontal gyrus, P3/P4 – supramarginal gyrus, T5/T6 – caudal anterior cingulate cortex. These cortical structures affect the activity of the vagus and sympathetic nuclei.

Figures 1 and 2 show that the use of balm causes a shift in the information field of the discriminant roots of the GDV, HRV and EEG parameters to the left and up. The shift to the left reflects, first of all, the normalizing decrease of increased sympathotonic markers and the increase of decreased vagotonic markers.

This is in line with the concept we put forward back in 1993 about ambivalence-equilibratory character of influence on organism of human of curative water Naftussya [8], which is now considered a generally accepted adaptogen [1,11,12,15,26,28,46,47,51].

Physiologically favorable vegetotropic effects of the balm are accompanied by a further increase in the initially increased activity of **beta-rhythm**-generating cortical and subcortical structures as well as activation of **theta-rhythm**-generating and inhibition of **alpha**- and **delta**-rhythm-generating nuclei whose initial activity was within normal limits.

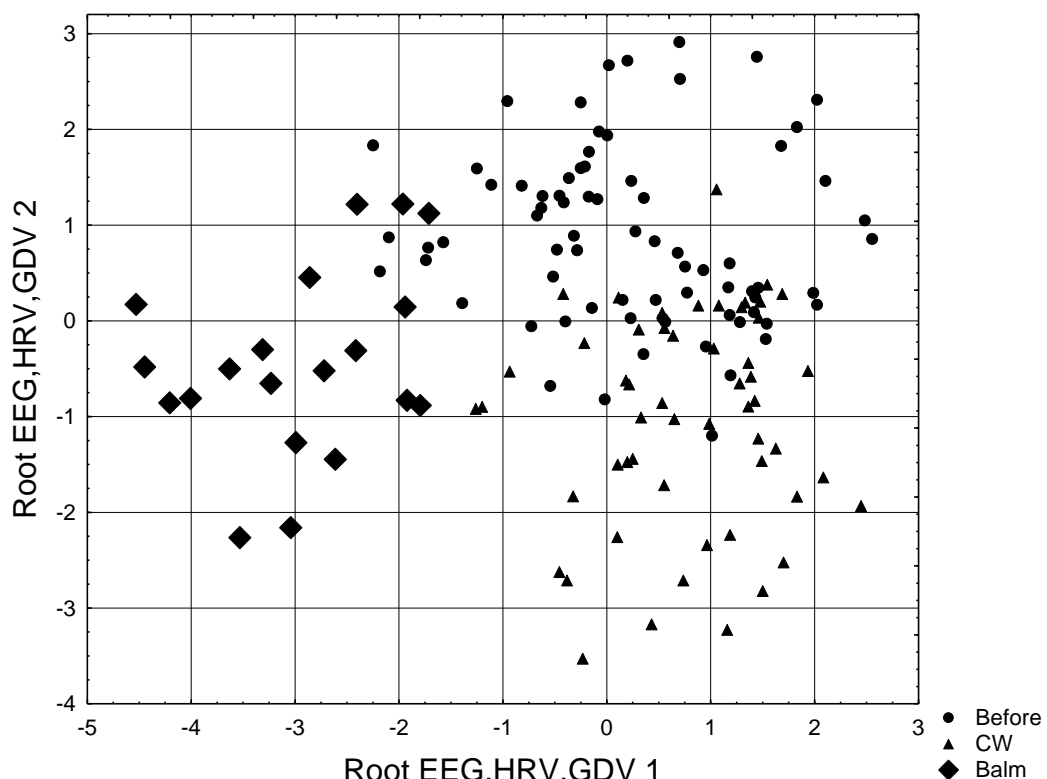


Fig. 1. Individual values of the first and second the GDV, EEG and HRV roots of the patients before (Baseline) and 1,5 hours after application of Control Water or Balm

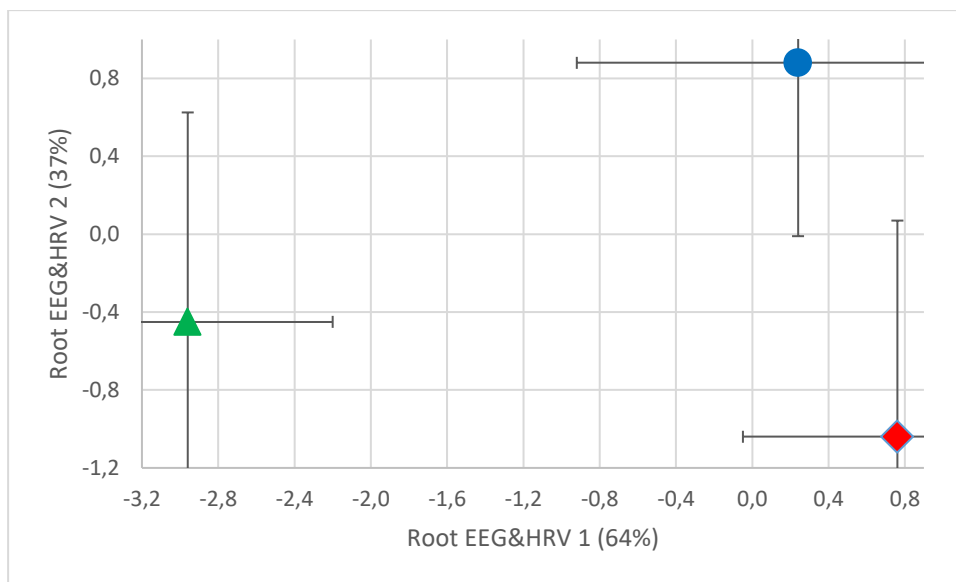


Fig. 2. Average (Mean±SD) of the first and second GDV, EEG and HRV roots of the patients before and 1,5 hours after application of control water or balm

The neurotropic effects of the balm are accompanied by significant changes in a number of GDV parameters. First of all, it is a decrease in the initially normal values of GDI fractality in the right and frontal projections and entropy in the right projection in combination with an increase in the GDI area in the right projection. It is important that the entropy of HRV decreases and the entropy of EEG in occipital loci increases. The physiological essence of entropy is discussed in detail in a recent monograph [13].

The biophysical and informational/mathematical essence of these parameters is unquestionable for unbiased scientists. Chakra issues remain debatable, in our opinion, **for now**. It will be recalled that even until the mid-1960s, the “most advanced Soviet science” denied the existence of genes (???).

We found that after applying the balm, the energy of the *virtual* first, fourth, fifth and seventh chakras increases significantly. And now let's remember that **fourth** and **fifth** Chakras associated with vagus nerve [10], the tone of which increases; **first** Chakra is associated with adrenals, consistent with increased PSD of ULF band as a marker of circulating catecholamines and glucocorticoids; **seventh** Chakra associated with **right** (paired EEG loci!) and upper brain [10].

The previously identified effects of the balm on the parameters of immunity and hemodynamics [1,11,12,15,26,34] are consistent with the notion that **fourth** Chakra is associated with thymus, celiac and cardial plexus, heart, circulation [10,48]. It is appropriate to mention the research data of our laboratory on the relationship between the parameters of EEG &HRV and immunity, as well as their changes under the influence of adaptogenic factors of the resort of Truskavets’ [29-33, 39-47].

Based on the fact that the balm activates the **fifth** Chakra, we risk predicting its short-term thyrotropic effect, as shown for Naftussya bioactive water [27,28].

The cluster of individuals in the control group was shifted along the axis of the first root in the opposite direction, which reflects the sympathotonic shift of autonomous balance and opposite changes in EEG parameters. It is unlikely that the reason for such changes in neurodynamics is the use of 50 ml of tap water. The neurotropic effects of individuals' occupational activity within 1,5 hours between tests and/or the ultradian biorhythm of the autonomic nervous system and cortisol are more obvious.

Interestingly, slight displacements along the axis of the second root were almost the same in both groups.

In general, all GDV&EEG&HRV clusters on the planes of two roots are quite clearly delineated, which is documented by calculating the Mahalanobis distances (Table 6).

Table 6. Squared Mahalanobis Distances between EEG&HRV Clusters, F-values (df=39) and p-levels

Groups	Base-line (74)	After CW (54)	After Balm (20)
Baseline (74)	0	4,80	12,48
After CW (54)	2,83 10^{-4}	0	15,07
After Balm (20)	3,72 10^{-6}	4,16 10^{-6}	0

The same discriminant parameters can be used to identify the belonging of one or another person to one or another cluster. This purpose of discriminant analysis is realized with the help of classifying (discriminant) functions (Table 7).

Table 7. Coefficients and Constants for Classification Functions

Clusters	Base-line (74)	After CW (54)	After Balm (20)
Variables	p=.500	p=,365	p=,135
ULF/TP, %	-3,715	-3,497	-3,898
F3-α PSD, %	-1,323	-1,338	-1,576
P4-δ PSD, %	2,082	2,017	1,769
C4-β PSD, $\mu\text{V}^2/\text{Hz}$	-0,059	-0,067	0,060
Ch2 Asymmetry	-82,42	-80,78	-81,02
T4-β PSD, $\mu\text{V}^2/\text{Hz}$	-0,005	-0,028	-0,065
Fp1-α PSD, %	0,467	0,372	0,488
P4-δ PSD, $\mu\text{V}^2/\text{Hz}$	0,182	0,217	0,215
LF/HF	4,406	4,551	4,624
Asymmetry-β, %	-0,176	-0,229	-0,177
O2-θ PSD, %	0,587	0,595	0,881
Frequency-β, %	-0,412	-0,523	-0,835
O1-θ PSD, $\mu\text{V}^2/\text{Hz}$	0,242	0,232	0,210
C3-α PSD, %	1,760	1,976	1,940
Ch5 Energy	-59,01	-52,98	-48,47
T6-α PSD, %	1,948	1,943	1,804
C4-β PSD, %	-0,381	-0,317	-0,551
P3-β PSD, %	4,229	4,191	4,409
Entropy HRV	429,2	427,8	443,2
HF PSD, msec²	-0,013	-0,014	-0,015
Ch1 Energy	-95,01	-102,8	-98,87
T3-α PSD, $\mu\text{V}^2/\text{Hz}$	0,042	0,038	0,018
F3-α PSD, $\mu\text{V}^2/\text{Hz}$	-0,192	-0,216	-0,199
O2-α PSD, $\mu\text{V}^2/\text{Hz}$	0,024	0,028	0,028
O2-α PSD, %	-0,670	-0,729	-0,718
T6-β PSD, %	1,106	1,193	1,261
T4-β PSD, %	-0,541	-0,645	-0,721
RMSSD, msec	-0,689	-0,904	-0,657
pNN₅₀, %	3,469	3,726	3,449
F3-β PSD, $\mu\text{V}^2/\text{Hz}$	0,070	0,101	0,078

Asymmetry-θ, %	0,487	0,443	0,471
Shape C Right	16,86	15,99	16,28
Shape C Frontal	8,862	9,298	9,383
O1-β PSD, %	-0,926	-0,853	-0,893
Area GDI R, kpixels	65,89	66,04	67,01
T3-α PSD, %	1,387	1,498	1,541
Entropy O1	187,2	193,3	181,5
O1-θ PSD, %	-4,974	-5,080	-4,653
Ch7 Energy	-199,2	-196,8	-205,3
Constants	-1463	-1466	-1500

In this case, we can retrospectively recognize members in the initial state with 8 errors, after using control water - with 8 errors, and after applying the balm - with 2 errors. Overall classification accuracy is 87,8% (Table 8). This is 6.7% higher than in our previous study [50].

Table 8. Classification Matrix for EEG&HRV Clusters

Rows: Observed classifications; Columns: Predicted classifications

	Clusters	Base-line	After CW	After Balm
Clusters	% Correct	p=.500	p=.365	p=.135
Baseline (74)	89,2	66	8	0
After CW (54)	85,2	8	46	0
After Balm (20)	90,0	2	0	18
Total	87,8	76	54	18

The digital data of Table 5 are visualized in Figure 3.

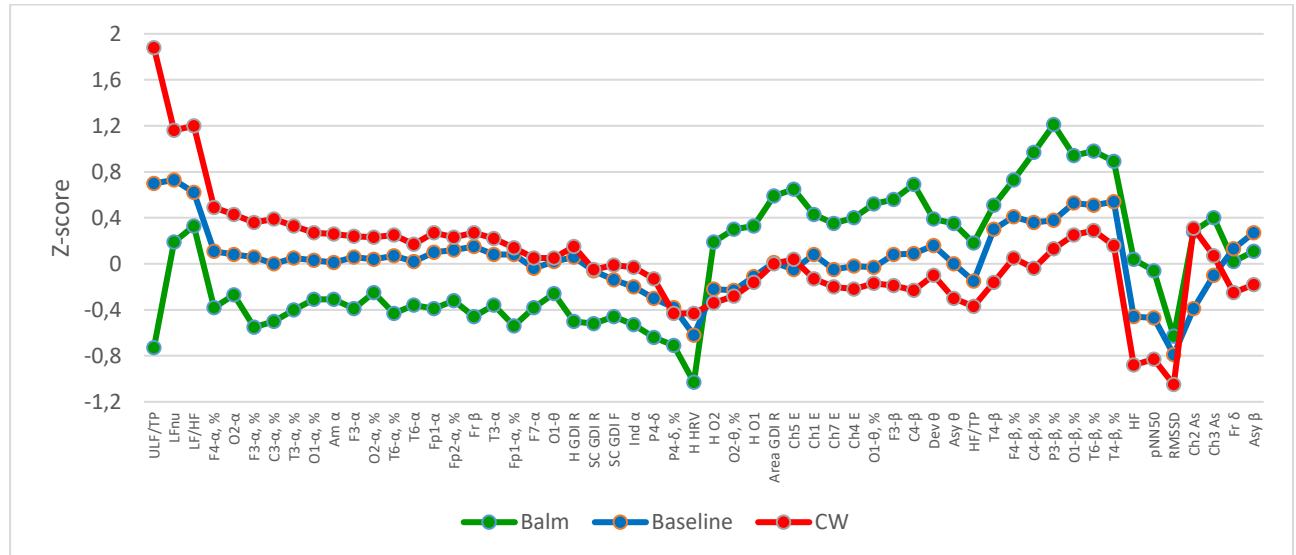


Fig. 3. Profiles of Z-scores of EEGs and HRVs variables in the initial state and 1,5 hours after drinking control water or balm

A clear divergence of profiles is visible, however, it is heterogeneous. Therefore, for more detailed analysis, the profiles were structured in 9 homogeneous patterns. This approach also makes it possible to model the own (per se) neurotropic effects of the balm as algebraic sums of effects in the main and control groups.

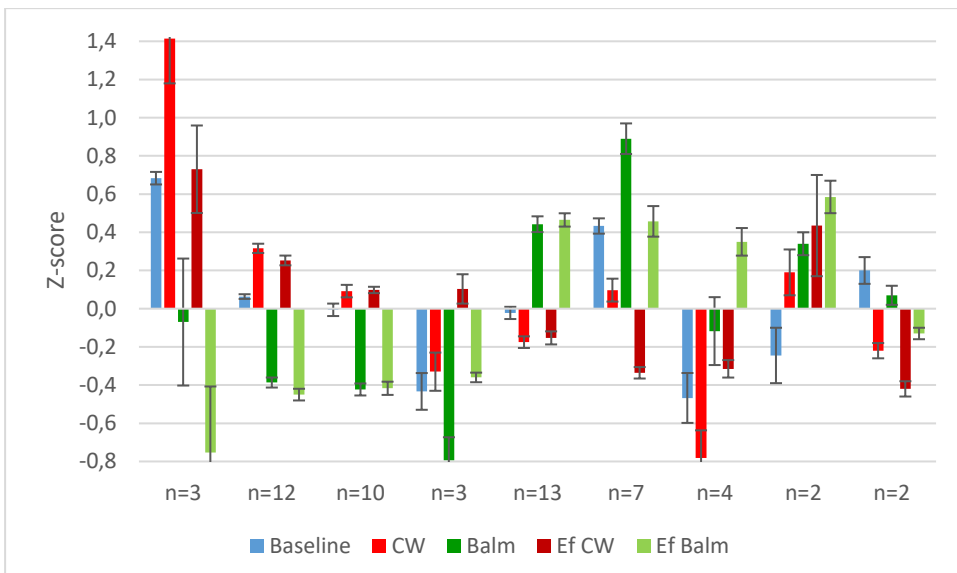


Fig. 4. Patterns of GDV, EEG and HRV (Mean±SE) parameters before and 1,5 hours after application of control water or balm and simulated effects per se. The members of the patterns are separated in table 5 by spaces

Regarding the factors of neurotropic effects of the balm, it is possible to assume the presence of polyphenols, which are present in both the balm [1,36,37] and bioactive water Naftussya [17], whose neurotropic and endocrine effects are well known [11,12,15,26,28,46,47].

ACKNOWLEDGMENT

We express sincere gratitude to GI Dubkova and TA Korolyshyn as well as administration of clinical sanatorium “Moldova” for help in recording GDV, EEG and HRV. Special thanks to the volunteers.

ACCORDANCE TO ETHICS STANDARDS

Tests in patients are conducted in accordance with positions of Helsinki Declaration 1975, revised and complemented in 2002, and directive of National Committee on ethics of scientific researches. During realization of tests from all participants the informed consent is got and used all measures for providing of anonymity of participants.

REFERENCES

1. Alyeksyeyev OI, Popovych IL, Panasyuk YeM, Barylyak LG, Sarancha SN, Shumakov MF. Adaptogens and Radiation [in Ukrainian]. Kyiv. Naukova dumka; 1996: 126.
2. Babelyuk VE, Gozhenko AI, Dubkova GI, Babelyuk NV, Zukow W, Kovbasnyuk MM, Popovych IL. Causal relationships between the parameters of gas discharge visualization and principal neuroendocrine factors of adaptation. Journal of Physical Education and Sport. 2017; 17(2): 624-637.
3. Babelyuk VYe, Popadynets' OO, Dubkova GI, Zukow W, Muszkieta R, Gozhenko OA, Popovych IL. Entropy of gas-discharge image correlates with the entropies of EEG, immunocytogram and leukocytogram but not HRV. Pedagogy and Psychology of Sport. 2020; 6(2): 30-39.
4. Babelyuk VYe, Gozhenko AI, Dubkova GI, Zukow W, Hubyts'kyi VY, Ruzhylo SV, Fedyayeva SI, Kovalchuk HY, Popovych IL. Causal relationships between the parameters of gas discharge visualization and immunity. Pedagogy and Psychology of Sport. 2021; 7(1): 115-134.

5. Babelyuk VY, Gozhenko AI, Dubkova GI, Babelyuk NV, Zukow W, Kindzer BM, Kovbasnyuk MM, Popovych IL. Causal relationships between the parameters of gas discharge visualization and phagocytosis. *Journal of Education, Health and Sport*. 2021; 11(6): 268-276.
6. Babelyuk VY, Tserkovnyuk RG, Ruzhylo SV, Dubkova GI, Babelyuk NV, Zukow W, Popovych IL. Causal relationships between the parameters of gas discharge visualization and leukocytogram. *Journal of Education, Health and Sport*. 2021; 11(7): 258-269.
7. Baevskiy RM, Ivanov GG. Heart Rate Variability: theoretical aspects and possibilities of clinical application [in Russian]. *Ultrazvukovaya i funktsionalnaya diagnostika*. 2001; 3: 106-127.
8. Balanovs'kyi VP, Popovych IL, Karpynets' SV. About ambivalence-equilibratory character of influence of curative water Naftussya on organism of human [in Ukrainian]. *Dopovidi ANU. Mat pryr tekhn nauky*. 1993; 3: 154-158.
9. Berntson GG, Bigger JT jr, Eckberg DL, Grossman P, Kaufman PG, Malik M, Nagaraja HN, Porges SW, Saul JP, Stone PH, Van der Molen MW. Heart Rate Variability: Origines, methods, and interpretive caveats. *Psychophysiology*. 1997; 34: 623-648.
10. Chase CR. The Geometry of Emotions: Using Chakra Acupuncture and 5-Phase Theory to Describe Personality Archetypes for Clinical Use. *Med Acupunct*. 2018; 30(4): 167-178.
11. Flyunt IS, Chebanenko OI, Hrinchenko BV, Barylyak LG, Popovych IL. *Balneophytoradiodefensology. Influence of therapeutic factors of Truskavets' spa on the state of adaptation and protection systems of the victims of the Chernobyl disaster* [in Ukrainian]. Kyiv. Computerpress; 2002: 112.
12. Flyunt IS, Chebanenko LO, Chebanenko OI, Kyjenko VM, Fil' VM. *Experimental Balneophytotherapy* [in Ukrainian]. Kyiv. UNESCO-SOCIO; 2008: 196.
13. Gozhenko AI, Korda MM, Popadynets' OO, Popovych IL. Entropy, Harmony, Synchronization and Their Neuro-Endocrine-Immune Correlates [in Ukrainian]. Odesa. Feniks; 2021: 232.
14. Heart Rate Variability. Standards of Measurement, Physiological Interpretation, and Clinical Use. Task Force of ESC and NASPE. *Circulation*. 1996; 93(5): 1043-1065.
15. Hrinchenko BV. Adaptive balneophytotherapy as a sanogenetic basis for rehabilitation of neuro-endocrine-immune system dysfunction [in Ukrainian]. *Medical Hydrology and Rehabilitation*. 2008; 6(1): 85-97.
16. Iseger TA, van Bueren NER, Kenemans JL, Gevirtz R, Arns M. A frontal-vagal network theory for Major Depressive Disorder: Implications for optimizing neuromodulation techniques. *Brain Stimul*. 2020; 13(1): 1-9.
17. Ivassivka SV, Bubnyak AB, Kovbasnyuk MM, Popovych IL. Genesis and role of phenols in waters from Naftussya layer [in Ukrainian]. In: *Problems of pathology in experiment and clinic. Scientific works of Drohobych Medical Institute. Vol XV*. Drohobych. 1994: 6-11.
18. Khaspekova NB. Diagnostic informativeness of monitoring HRV [in Russian]. *Vestnik aritmologii*. 2003; 32: 15-23.
19. Khayutin VM, Lukoshkova EV. Spectral analysis of the heart rate oscillations: physiological foundation and complicating it phenomena [in Russian]. *Russian Journal of Physiology*. 1999; 85(7): 893-909.
20. Klecka WR. Discriminant Analysis [trans. from English in Russian] (Seventh Printing, 1986). In: *Factor, Discriminant and Cluster Analysis*. Moskva. Finansy i Statistika; 1989: 78-138.
21. Korkushko OV, Pysaruk AV, Shatylo VB. The value of heart rate variability analysis in cardiology: age aspects [in Russian]. *Circulation and Hemostase*. 2009; 1-2: 127-139.
22. Korotkov KG. Basics GDV Bioelectrography [in Russian]. SPb. SPbGITMO(TU); 2001: 360.
23. Korotkov KG. Principles of Analysis in GDV Bioelectrography [in Russian]. SPb. Renome; 2007: 286.
24. Korotkov KG. Energy Fields Electrophotonic Analysis in Humans and Nature. Second updated edition. Translated from Russian by the author. Edited by Berney Williams and Lutz Rabe. 2014: 233.
25. Kotelnikov SA, Nozdrachov AD, Odinak MM, Shustov EB, Kovalenko IYu, Davidenko VYu. Heart rate variability: understanding of the mechanisms [in Russian]. *Fiziologiya cheloveka*. 2002; 28(1): 130-143.
26. Kostyuk PG, Popovych IL, Ivassivka SV (Editors). *Chornobyl, Adaptive and Protection*

- Systems, Rehabilitation. Adaptive, metabolic, hemostasis and immunological aspects of diagnostics and balneo- and phytorehabilitation in Truskavets' spa of persons exposed to Chornobyl accident factors [in Ukrainian]. Kyiv. Computerpress; 2006: 348.
27. Kozyavkina NV, Gozhenko AI, Barylyak LG., Korolyshyn TA, Popovych IL. Variety immediate thyrotropic effects of bioactive water Naftussya, their neuroendocrine-immune accompaniment and possibility of forecast [in Ukrainian]. Medical Hydrology and Rehabilitation. 2013; 11(4): 27-54.
28. Kozyavkina OV, Kozyavkina NV, Gozhenko OA, Gozhenko AI, Barylyak LG., Popovych IL. Bioactive Water Naftussya and Neuro-Endocrine-Immune Complex [in Ukrainian]. Kyiv. UNESCO-SOCIO; 2015: 349.
29. Kozyavkina OV, Popovych IL, Zukow W. Immediate vegetotropic effects of bioactive water Naftussya and their neuro-endocrine-immune accompaniment in healthy men. Journal of Health Sciences. 2013; 3(5): 391-408.
30. Kul'chyn's'kyi AB, Gozhenko AI, Zukow W, Popovych IL. Neuro-immune relationships at patients with chronic pyelonephritis and cholecystitis. Communication 3. Correlations between parameters EEG, HRV and Immunogram. Journal of Education, Health and Sport. 2017; 7(3): 53-71.
31. Kul'chyn's'kyi AB, Kovbasnyuk MM, Korolyshyn TA, Kyjenko VM, Zukow W, Popovych IL. Neuro-immune relationships at patients with chronic pyelonephrite and cholecystite. Communication 2. Correlations between parameters EEG, HRV and Phagocytosis. Journal of Education, Health and Sport. 2016; 6(10): 377-401.
32. Kul'chyn's'kyi AB, Kyjenko VM, Zukow W, Popovych IL. Causal neuro-immune relationships at patients with chronic pyelonephritis and cholecystitis. Correlations between parameters EEG, HRV and white blood cell count. Open Medicine. 2017; 12(1): 201-213.
33. Kul'chyn's'kyi AB, Zukow W, Korolyshyn TA, Popovych IL. Interrelations between changes in parameters of HRV, EEG and humoral immunity at patients with chronic pyelonephritis and cholecystitis. Journal of Education, Health and Sport. 2017; 7(9): 439-459.
34. Markova OO, Popovych IL, Tserkovnyuk AV, Barylyak LG. Adrenaline myocardiodystrophy and reactivity of the organism [in Ukrainian]. Kyiv. Computerpress; 1997: 126.
35. Newberg AB, Alavi A, Baime M, Pourdehnad M, Santanna J, d'Aquili E. The measurement of regional cerebral blood flow during the complex cognitive task of meditation: a preliminary SPECT study. Psychiatry Research: Neuroimaging Section. 2001; 106: 113-122.
36. Panasyuk YM, Levkut LH, Popovych IL, Alekseyev OI, Kovbasnyuk MM, Balanovskyi VP. Experimental study of adaptogenic properties of "Crimean" balm [in Ukrainian]. Fiziol Zh. 1994; 40(3-4): 25-30.
37. Pat. 10271 Ukraine MKI A 61 K 31/00. Adaptogenic agent [in Ukrainian]. Panasyuk YM, Levkut LG, Popovych IL, Shumakov MF, Sychova AO, Alekseyev OI, Bakova MM. 1996. Bull № 4.
38. Popovych IL. The concept of neuro-endocrine-immune complex (review) [in Russian]. Medical Hydrology and Rehabilitation. 2009; 7(3): 9-18.
39. Popovych IL. Immediate responses of the autonomic nervous system to the balneofactors, their neuro-endocrine-immune accompaniments and predictors. Experimental and Clinical Physiology and Biochemistry. 2018; 1(81): 11-26.
40. Popovych IL, Gozhenko AI, Zukow W, Polovynko IS. Variety of Immune Responses to Chronic Stress and their Neuro-Endocrine Accompaniment. Scholars' Press. Riga; 2020: 172.
41. Popovych IL, Kozyavkina OV. Immediate vegetotropic effects of bioactive water Naftussya and their neuro-endocrine-immune accompaniment in apparently healthy men [in Ukrainian]. Medical Hydrology and Rehabilitation. 2012; 10(3): 32-65.
42. Popovych IL, Kozyavkina OV, Kozyavkina NV, Korolyshyn TA, Lukovych YuS, Barylyak LG. Correlation between Indices of the Heart Rate Variability and Parameters of Ongoing EEG in Patients Suffering from Chronic Renal Pathology. Neurophysiology. 2014; 46(2): 139-148.
43. Popovych IL, Kul'chyn's'kyi AB, Korolyshyn TA, Zukow W. Interrelations between changes in parameters of HRV, EEG and cellular immunity at patients with chronic pyelonephritis and cholecystitis. Journal of Education, Health and Sport. 2017; 7(10): 11-23.
44. Popovych IL, Kul'chyn's'kyi AB, Gozhenko AI, Zukow W, Kovbasnyuk MM, Korolyshyn TA.

- Interrelations between changes in parameters of HRV, EEG and phagocytosis at patients with chronic pyelonephritis and cholecystitis. Journal of Education, Health and Sport. 2018; 8(2): 135-156.
45. Popovych IL, Lukovych YuS, Korolyshyn TA, Barylak LG, Kovalska LB, Zukow W. Relationship between the parameters heart rate variability and background EEG activity in healthy men. Journal of Health Sciences. 2013; 3(4): 217-240.
 46. Popovych IL, Ruzhylo SV, Ivassivka SV, Aksentiychuk BI (Editors). Balneocardioangiology [in Ukrainian]. Kyiv. Computerpress; 2005: 229.
 47. Popovych IL, Vis'tak HI, Gumege MD, Ruzhylo SV. Vegetotropic Effects of Bioactive Water Naftussya and their Endocrine-Immune, Metabolic and Hemodynamic Accompaniments [in Ukrainian]. Kyiv. UNESCO-SOCIO; 2014: 163.
 48. Puchko LG. Multidimensional Medicine. System of Self-diagnosis and Self-healing of Human [in Russian]. 10th ed. rev. and ext. Moskva. ANS: 2004: 432.
 49. Romodanov AP (Editor). Postradiation Encephalopathy. Experimental Researches and Clinical Observations [in Ukrainian and Russian]. Kyiv. USRI of Neurosurgery; 1993: 224.
 50. Ruzhylo SV, Fihura OA, Zukow W, Popovych IL. Immediate neurotropic effects of Ukrainian phytocomposition. Journal of Education, Health and Sport. 2015; 5(4): 415-427.
 51. Ruzhylo SV, Tserkovnyuk AV, Popovych IL. Actotrophic Effects of Balneotherapeutic Complex of Truskavets' spa [in Ukrainian]. Kyiv. Computerpress; 2003: 131.
 52. Shaffer F, Ginsberg JP. An Overview of Heart Rate Variability Metrics and Norms. Front Public Health. 2017; 5: 258.
 53. Shannon CE. A mathematical theory of information. Bell Syst Tech J. 1948; 27: 379-423.
 54. Winkelmann T, Thayer JF, Pohlak ST, Nees F, Grimm O, Flor H. Structural brain correlates of heart rate variability in healthy young adult population. Brain Structure and Function. 2017; 222(2): 1061-1068.
 55. Yoo HJ, Thayer JF, Greenig S, Lee TH, Ponzio A, Min J, Sakaki M, Nga L, Mater M, Koenig J. Brain structural concomitants of resting state heart rate variability in the young and old: evidence from two independent samples. Brain Structure and Function. 2018; 223(2): 727-737.